On-Line Adaptation of Wall-Wetting Model Parameters

Conference Paper · September 2001

5 authors, including:

Alessandro di Gaeta
Italian National Research Council

Luigi Glielmo
University of Sannio

Stefania Santini
University of Naples Federico II

On-Line Adaptation of Wall-Wetting Model Parameters

Alessandro di Gaeta,⋆ Luigi Glielmo,• Stefania Santini⋆
Vittorio Cioffi,† and Carlo Di Giuseppe†

⋆ *Dipartimento di Informatica e Sistemistica, Università di Napoli Federico II*
{digaeta, stsantin}@unina.it
• *Facoltà di Ingegneria, Università del Sannio in Benevento*
glielmo@unisannio.it
† *ELASIS, Società di Ricerca del gruppo FIAT nel Mezzogiorno*
{vittorio.cioffi, carlo.digiuseppe}@elasis.fiat.it

Abstract

Spark-ignited engines equipped by a three-way catalyst require a precise control of the air fuel ratio (A/F) fed to the combustion chamber. A stoichiometric mixture is necessary for the proper working of the catalyst in order to meet the legislation requirement.

A critical part of the A/F control is the feed-forward compensation of the fuel dynamics. Conventional strategies are based on a simplified model of the wall-wetting phenomena whose parameter values (the well known X and τ_f in the Aquino's model) are stored in off-line computed look-up tables. Unfortunately, different factors such as aging of the engine components, wide range of possible fuels, errors in the parameters calibration over the whole engine map deteriorate the control performances in terms of emissions.

In this paper, we present a strategy for the slow on-line adaptation of the wall-wetting dynamics. In particular the algorithm detects when parameter mismatch occurs and then uses a least squares method to perform the adaptation. The aim is to reduce temporary lean (rich) excursions during fast accelerations (decelerations), and obtain a good compensation during rapid throttle transients.

The whole procedure was designed and tested by numerical simulations based on experimental data.

1 Introduction

Port fuel injected gasoline engines, equipped by three-way catalytic converters, require the tight control of the mixture fed to the cylinders. As well known, the converter chemically enables the removal of carbon monoxide, oxides of nitrogen and hydrocarbons, but to let the catalyzed reactions proceed simultaneously with a satisfactory efficiency, the A/F mixture has to be stoichiometric.

In current technology for gasoline car, the signal of an oxygen sensor (λ-sensor), placed on the exhaust pipe, is used as a feedback control signal for the fuel injection system in order to ensure stoichiometry of the mixture (see, for example [3]). These current strategies employ simplified dynamic models of the engine behavior based on off-line look-up tables (engine maps).

A typical fuel control system is composed by a feed-back control and a feed-forward action for the proper compensation of fuel dynamics (see figure 1). Fuel and air dynamics, the presence of transport delays, and slow sensor characteristics, make the A/F control slow in ensuring stoichiometry. The limitate bandwidth of the feedback loop [2] makes thus appropriate to improve the design of the feed-forward action.

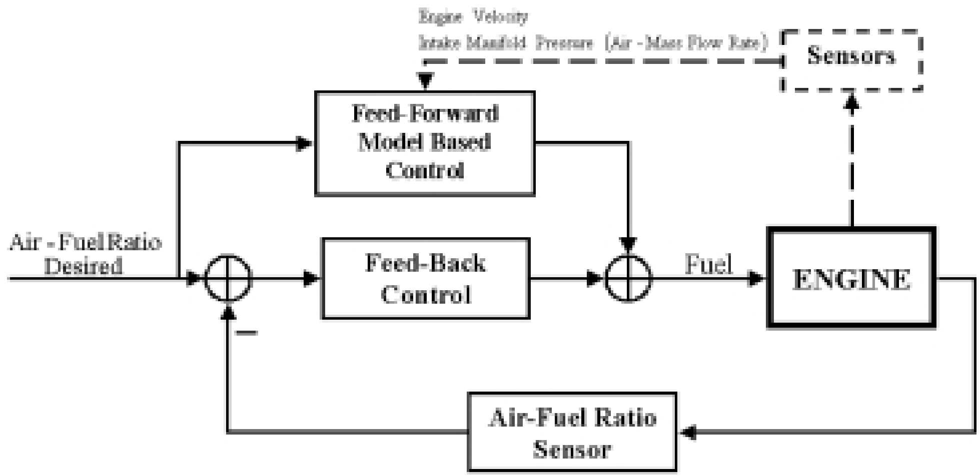

Figure 1: Schematics of a fuel control system.

In this paper an on-line adaptation of wall-wetting parameters is presented. During normal engine operations, the algorithm is enabled when an undesirable excursion in the A/F value occurs. In these conditions a least squares method is used to perform the refinement of the model based compensator parameters. The adaptive strategy also updates the look-up table in which the parameters are stored. The adjusted parameters will allow a reduction in the A/F excursion for the next transients.

2 The Fuel Film Compensator

The tuning of the feed-forward compensation is crucial to limit air-fuel excursion: indeed if they are not well captured, the fuel dynamics can cause undesirable excursion, during opening and closing operation of the throttle, and so they are directly responsible of pollution. The mixture formation process is well known as the source of the A/F problems and therefore will be only briefly introduced here.

In figure 2, the main characteristics of the fuel dynamics (the so called wall wetting phenomena) are summarized. The fuel is sprayed in the intake manifold (intake runner). Some of the fuel immediately feeds the cylinder, while the rest contributes to the formation of a fuel film on the intake manifold wall and/or on the valve body. Liquid from the puddle evaporates through time, thus participating to the mixture formation process and entering the cylinder. The evaporation process depends on the mass of the puddle, manifold pressure, wall and valve temperatures, and back-flow phenomena [4, 10].

Usually, for control applications the engine behavior is described by a Mean Value Engine Model (MVEM) (see, for example [6] and reference therein). The goal of this modeling technique is to represent the dynamics of the overall engine behavior on a time scale of several engine events with an overall accuracy of 1 to 3 percent. In other

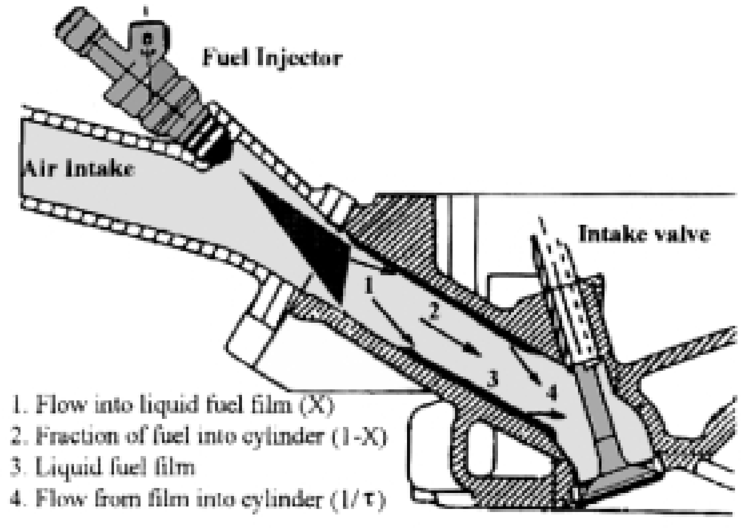

Figure 2: Schematics of the fuel dynamics.

words, the model has to be phenomenological, consistent, compact, with just a minimum number of fitting parameters, so as to be easily adaptable to different engines.

Following this approach, the simplest fuel flow model of the MVEM can be written according to Aquino [1] (see also figure 2):

$$\dot{m}_{ff} = -\frac{1}{\tau_f} m_{ff} + X \dot{m}_{fi} \tag{1a}$$

$$\dot{m}_{fc} = \frac{1}{\tau_f} m_{ff} + (1-X) \dot{m}_{fi} \tag{1b}$$

where m_{ff} is the fuel mass of the puddle, $\dot{m}_{fi}$ is the injected fuel mass flow rate, $\dot{m}_{fc}$ is the mass flow rate of the fuel incoming the cylinder; X is a parameter representative of the fraction of injected fuel that goes into the puddle; τ_f parameter describes the evaporation from the puddle. Notice that, at the low temperatures, some of the liquid fuel from the puddle directly enters in the combustion chamber and τ_f can be chosen as representative of this phenomenon too.

The normalized fuel-air ratio can be defined as

$$\phi_c = S \frac{\dot{m}_{fc}}{\dot{m}_{ac}}, \tag{2}$$

where S is the stoichiometric A/F, and $\dot{m}_{ac}$ is the air mass flow rate incoming the engine.

The current approach in the A/F control is to identify off-line the parameters X and τ_f on the whole engine map, store these values in look-up tables and then design the feed-forward action, inverting the fuel dynamics (1), as

$$T_{\mathrm{FF}}(s; X, \tau_f) = T_{\mathrm{fuel}}^{-1}(s; X, \tau_f) = \frac{(1+s\tau_f)}{1+s\tau_f(1-X)}, \tag{3a}$$

$$\dot{m}_{fi_{\mathrm{FF}}} = T_{\mathrm{FF}} \dot{m}_{fc_{\mathrm{DES}}} = T_{\mathrm{FF}} \frac{\dot{m}_{ac}}{S} \phi_{c_{\mathrm{DES}}} \tag{3b}$$

where $\phi_{c_{\mathrm{DES}}}$ is the desired fuel-air ratio, and $\dot{m}_{fi_{\mathrm{FF}}}$, $\dot{m}_{fc_{\mathrm{DES}}}$ are respectively, the injected fuel mass flow rate of the feed-forward and the desired in-cylinder fuel mass flow rate.

The fuel dynamics depend on many factors [1, 5, 7], such as manifold pressure, manifold and valve temperature, engine speed, puddle dimensions, fuel composition and volatility. Only some of them can be directly measured. The calibration activity have to ensure compensator robustness against all this various disturbances, thus resulting often suboptimal in emission reduction during transients.

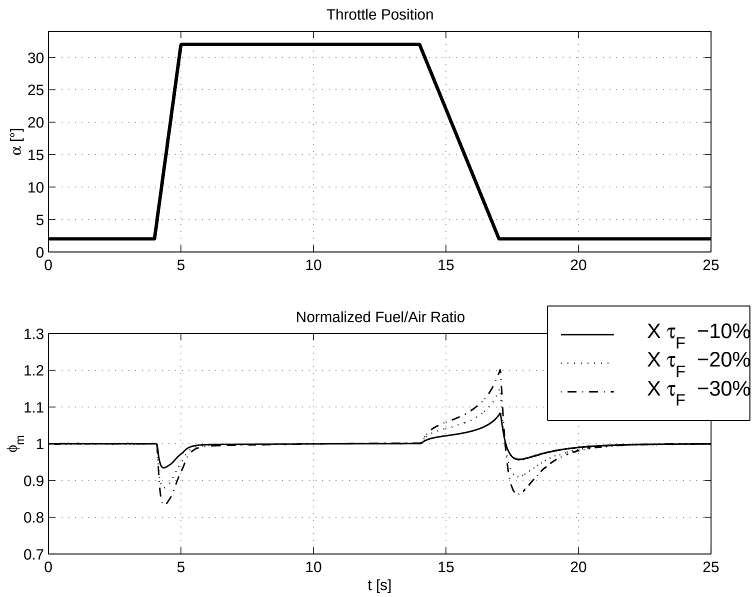

Figure 3: Normalized air fuel ratio excursion due to improper compensation of fuel dynamics. Graphics refer to a parameter mismatch of 10%, 20%, 30%.

Improprie compensation of wall-wetting dynamics, due to errors in the calibrating activity, changing dynamics caused by aging, and different fuel properties (in particular its volatility), contributes to a degrade in the effectiveness of the feed-forward action, and consequently in the emissions reduction (see figure 3) and in the driveability [11].

To avoid these problems in the following sections an on-line adaptation strategy for the X and τ_f parameters will be illustrated.

3 The Adaptive On-Line Strategy

The adaptive strategy is based on the monitoring of the A/F signal measured by a linear oxygen sensor in order to detect the occurrence of a badly compensated transients. It is performed according to the following steps:

- transient detection
- X and τ_f adaptation
- update of the X and τ_f look-up table

3.1 Transient Detection

As already mentioned, the goal of this work is the slow on-line adaptation of the wall-wetting dynamics during transients. The algorithm first detects when parameter mismatch occurs and then uses a least squares method to perform the adaptation.

A fundamental part of the strategy is the detection of those transients responsible of not negligible excursion of ϕ_c. Once detected, such transient is utilized to update the X and τ_f parameters by the adaptation procedure illustrated in the following section.

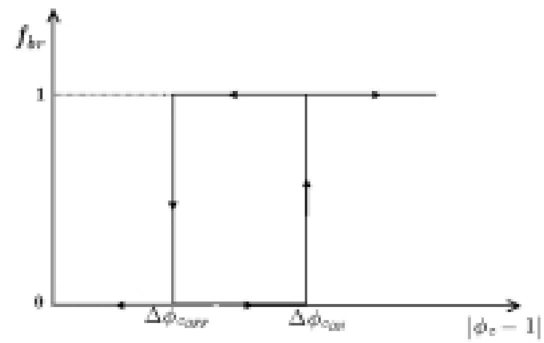

Figure 4: Binary relay function.

The transient detection strategy compute a binary signal ET (Enable Transient) that is high when a significative transient is recognized. The algorithm is simply based on the ϕ_c excursion:

$$ET = f_{br}(|\phi_c - 1|, \Delta\phi_{c_{ON}}, \Delta\phi_{c_{OFF}}) \tag{4}$$

where f_{br} is the binary relay function (see figure 4) with ON and OFF switch thresholds, respectively $\Delta\phi_{c_{ON}}$ and $\Delta\phi_{c_{OFF}}$. The algorithm uses ϕ_c measurements obtained by an EGO sensor placed in the exhaust pipe.

When the ET signal is high, samples of the signals $\dot{m}_{fi}, N, \phi_c, \dot{m}_{ac}, P_{man}$ are stored, where P_{man} is the intake manifold pressure. Notice that, the ET signal reset is ensured by the closed-loop action that guarantees the ϕ_c excursion become lower than $\phi_{c_{OFF}}$.

When the ET signal becomes low a further test is performed. Since ϕ_c excursion may be related not only to X and τ_f mismatch, but also to additive disturbances, such as misfire and cut-off [7]. In such conditions, the adaptation procedure is not applied. In order to establish the transient nature, the second check uses the P_{man} signal acquired. In particular the algorithm computes the pressure variation, compares it to a threshold ($\Delta_{P_{man}}$), and thus recognizes the air charge transient:

$$\max_{k \in [1 \ldots n]} P_{man} - \min_{k \in [1 \ldots n]} P_{man} > \Delta_{P_{man}}, \tag{5}$$

where n is the number of samples selected during the ET high duration. At the end of the transient detection phase the signals are used to build the regressor, as it will be explained in section 3.2.1.

Figures 5 show, as an example, a transient detection performed by the strategy.

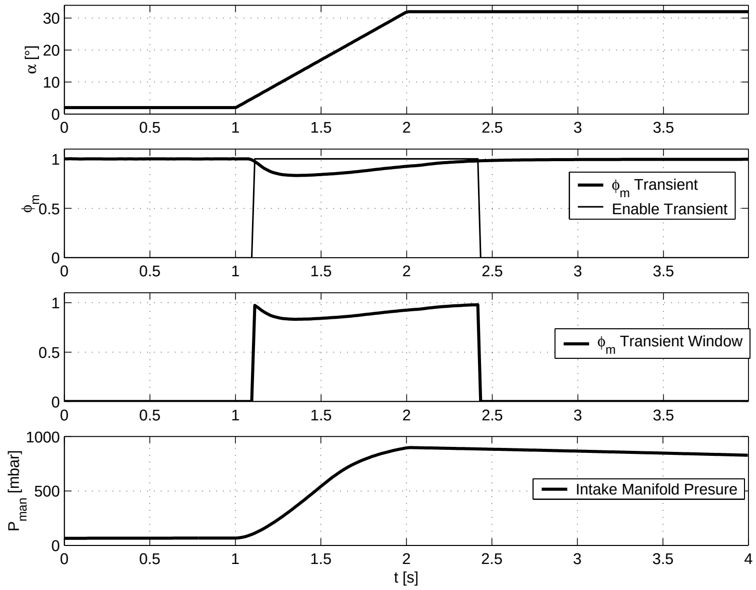

Figure 5: Transient detection dring throttle opening transient.

3.2 X and τ_f Adaptation

In the following the adaptation procedure will be illustrated, taking also into account the finite delay.

3.2.1 Least Square Estimation

The identification algorithm is based on the angle-based version of the Aquino's model (1):

$$\frac{dm_{ff}}{d\theta} = -\frac{1}{6N\tau_f} m_{ff} + \frac{X}{6N}\dot{m}_{fi} \tag{6a}$$

$$\dot{m}_{fc} = \frac{1}{\tau_f} m_{ff} + (1-X)\dot{m}_{fi} \tag{6b}$$

where θ is the crank-shaft angle, and N is the engine speed (r.p.m).

Equations (2) (6) can be now written together as

$$\frac{dm_{ff}}{d\theta} = -\frac{1}{6N\tau_f} m_{ff} + \frac{X}{6N}\dot{m}_{fi}, \tag{7a}$$

$$\phi_c = \frac{S}{\dot{m}_{ac}} \left(\frac{1}{\tau_f} m_{ff} + (1-X)\dot{m}_{fi} \right). \tag{7b}$$

From equation (7b), m_{ff} is:

$$m_{ff} = \tau_f \left[\frac{\dot{m}_{ac}}{S}\phi_c - (1-X)\dot{m}_{fi} \right]; \tag{8}$$

substituting equation (8) in (7a) the Aquino's model can be now rewritten in an input-output form as

$$\frac{d}{d\theta}\left\{ \tau_f \left[\frac{\dot{m}_{ac}}{S}\phi_c - (1-X)\dot{m}_{fi} \right] \right\} = -\frac{1}{6N\tau_f}\left\{ \tau_f \left[\frac{\dot{m}_{ac}}{S}\phi_c - (1-X)\dot{m}_{fi} \right] \right\} + \frac{X}{6N}\dot{m}_{fi}. \tag{9}$$

Defined the quantity z as

$$z \triangleq -\frac{\dot{m}_{ac}\phi_c}{S} + \dot{m}_{fi}; \tag{10}$$

equation (9) becomes

$$\frac{d}{d\theta}\left\{-\tau_f z + \tau_f X \dot{m}_{fi}\right\} = -\frac{1}{6N\tau_f}\left\{-\tau_f z + \tau_f X \dot{m}_{fi}\right\} + \frac{X}{6N}\dot{m}_{fi}. \tag{11}$$

Under the hypothesis that X and τ_f are slowly varying with respect to angle, equation (11) can be regarded as

$$-\tau_f \frac{dz(\theta)}{d\theta} + \tau_f X \frac{d\dot{m}_{fi}(\theta)}{d\theta} = \frac{z(\theta)}{6N(\theta)}. \tag{12}$$

Integrating the first and second member of equation (12) between θ_0 and θ and defining

$$s(\theta) = \int_{\theta_0}^{\theta}\left(\dot{m}_{fi}(\xi) - \frac{\dot{m}_{ac}(\xi)\phi_c(\xi)}{S}\right) d\xi = \int_{\theta_0}^{\theta} \frac{z(\xi)}{6N(\xi)} d\xi, \tag{13}$$

equation (12) can be easily rewritten as

$$s(\theta) = -\tau_f\left[z(\theta) - z(\theta_0)\right] + \tau_f X\left[\dot{m}_{fi}(\theta) - \dot{m}_{fi}(\theta_0)\right] \tag{14}$$

System identification algorithms require a certain amount of discrete data. For these reason, in order to find a linear regressor model, the function (14), linear in the unknown parameters τ_f, $\tau_f X$, have been discretized.

Defined $\theta_k = k\theta_c + \theta_0$, where $\theta_c = 180°$ is the sample time, the expression (14) becomes

$$s(k) = -\tau_f\left[z(k) - z(k_0)\right] + \tau_f X\left[\dot{m}_{fi}(k) - \dot{m}_{fi}(k_0)\right], \qquad \text{for} \quad k = 1, 2, \cdots, n. \tag{15}$$

where n is the number of measures defined in section 3.1.

Let now define

$$\begin{aligned}
S^T(n) &= [s(1) \cdots s(n)], & \text{(16a)}\\
\phi^T(k) &= [-(z(k) - z(k_0)) \quad (\dot{m}_{fi}(k) - \dot{m}_{fi}(k_0))], & \text{(16b)}\\
\Phi(n) &= \begin{bmatrix} \phi^T(1) \\ \cdot \\ \cdot \\ \cdot \\ \phi^T(n) \end{bmatrix}, & \text{(16c)}\\
\gamma &= \begin{bmatrix} \tau_f \\ \tau_f X \end{bmatrix}; & \text{(16d)}
\end{aligned}$$

from equation (15), the actual linear regression model can be now written as

$$s(k) = \phi^T(k)\gamma + e(k), \tag{17}$$

where $e(k)$ is the noise representative of the model and measure uncertainties.

Under the hypothesis of white noise, the optimal model predictor is given by [8, 9]

$$\hat{s}(k|\gamma) = \phi^T(k)\gamma. \tag{18}$$

while the prediction error is

$$e(k|\gamma) = s(k) - \hat{s}(k|\gamma). \tag{19}$$

The parameter estimation problem is to find a γ vector that minimize the sum-squared error:

$$\frac{1}{2}\sum_{k=1}^{n} e^2(k|\gamma). \tag{20}$$

The solution is a least-squares estimation [8, 9] of γ given by

$$\hat{\gamma} = (\Phi^T\Phi)^{-1}\Phi^T S. \tag{21}$$

From (21), the estimate of aquino's parameters can be obtained:

$$\hat{\tau}_f = \hat{\gamma}(1) \qquad \hat{X} = \frac{\hat{\gamma}(2)}{\hat{\gamma}(1)} \tag{22}$$

3.2.2 Introducing the Delay

Notice that the normalized equivalence fuel-air ratio, effectively measured by the EGO sensor, is a delayed version of the in cylinder ratio (see also figure 6):

$$\phi_m(\theta) = \phi_c(\theta - \theta_T). \tag{23}$$

θ_T is representative of both the injection, combustion and transport delay from the exhaust valve to the pre-catalyst sensor (see [2, 12], and reference therein, for more details):

$$\theta_T = \theta_{inj} + \theta_{burned} + \theta_{transport}, \tag{24}$$

where the injection delay θ_{inj} is sum of computation duration, injection duration, and injection timing; the θ_{burned} delay is, for a 4-stroke engine, is comprise in $[540°, 720°]$ (depending from the engine); and $\theta_{transport}$ delay depends on different variables such as engine velocity, exhaust air mass flow rate, exhaust temperature, let alone exhaust manifold geometric parameters such as volume and mean λ-sensor distance from outlet engine valves.

In presence of delay, the procedure exposed before is still applicable. As shown in figure 6, signal synchronization can be achieved by delaying (a θ_T late) all the variables needed to build the z and s function necessary in the regressor construction (see section 3.2.1).

A problem arises in the θ_T estimation. In this work, an average delay in function of the only engine speed has been considered. Better results could be achieved in future, by introducing a delay estimation in function of the engine operative point and/or using a technique to estimate the delay.

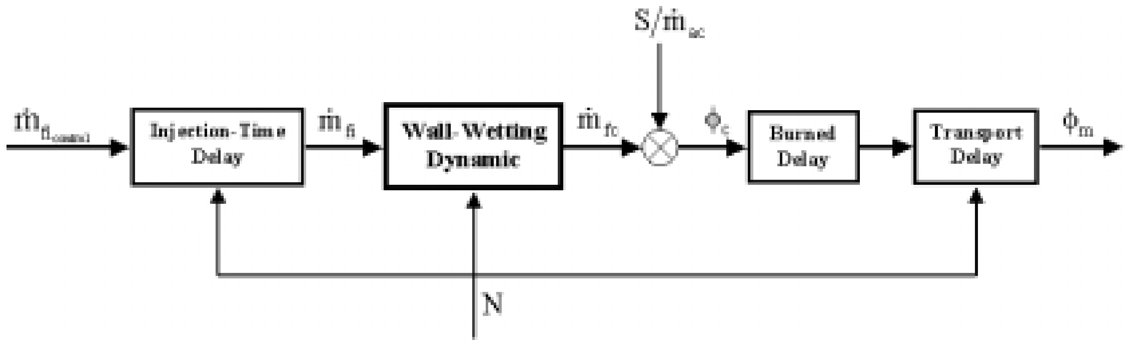

Figure 6: Open loop plant in presence of delays.

3.3 Update of the X and τ_f Look-Up Table

After the transient detection and the parameters estimation, it is necessary to update the X and τ_f look-up tables. Typically, the tables, resident in the electronic central unit (ECU), are stored in matrices indexed by intake manifold pressure (P_{man}), engine velocity (N) and intake manifold temperature (T_{man}).

Here we use a special look-up table to store the X, τ_f corrections. Each of the three entry point, necessary to update the matrix, is computed as the average value on the last m samples by the following transfer function

$$G(z) = \frac{1 - z^{-m}}{m(1 - z^{-1})}. \tag{25}$$

The output of the 'media filter' (25), at the beginning of the selected transient, will be used as matrix index.

4 Results

Figure 7 shows, as an example, the performances of the adaptive strategy in simulation. In the first frame the throttle transient is represented. The second frame illustrates the correspondent behavior of the fuel-air ratio measured at the exhaust pipe. The solid and the dotted line refer to the same transient respectively before and after X and τ_f adaptation. Notice that the closed-loop A/F control is active in both conditions. The adaptive strategy shows a good behavior in reducing the fuel-air excursion.

Figures 8 and 9 illustrate the effectiveness of the identification procedure. To this goal the measured ϕ_m is compared to the modeled ϕ. Notice that, the X and τ_f parameters of the Aquino model were identified using open-loop experimental data. It is apparent that the proposed technique could be used not only on-line, but also at the test bench during the calibration phase necessary for the X and τ_f look-up table building.

The identification procedure have been also tested in closed-loop conditions while the engine was controlled by an electronic control unit. Figure 10 shows, as an example, the model behavior against experimental data during a rapid tip-in tip-out (see figure 11 for the corresponding manifold pressure variation).

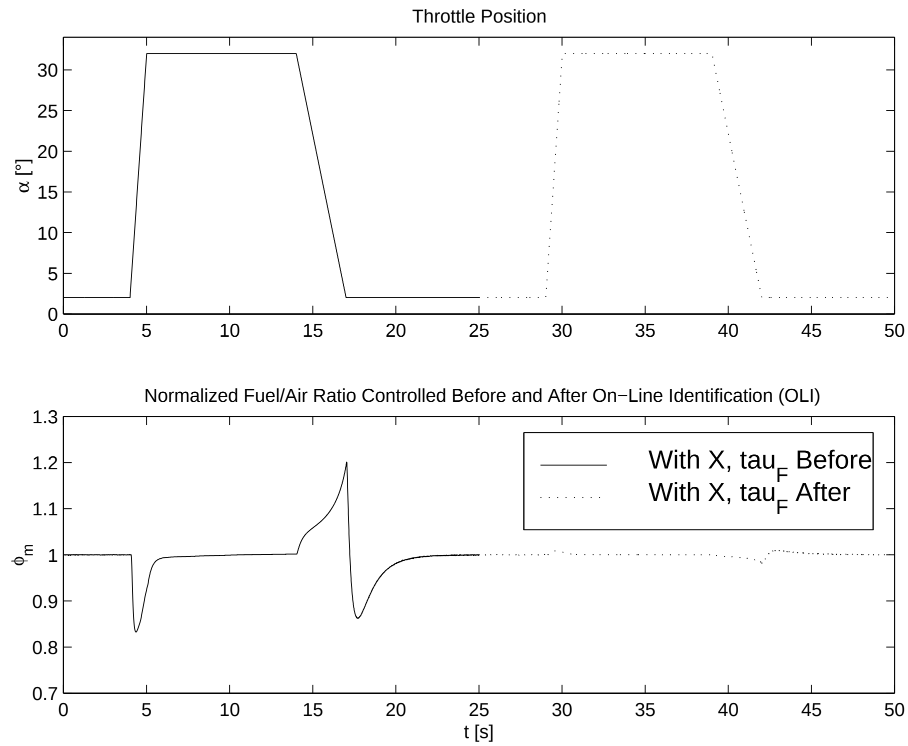

Figure 7: Normalized air-fuel ratio before and after the parameter adaptation.

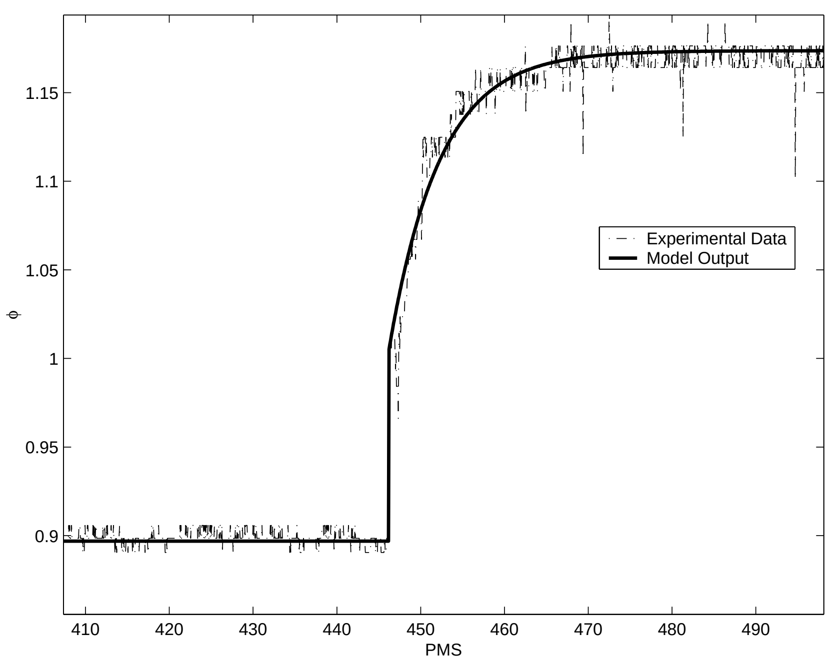

Figure 8: Normalized AIR/FUEL ratio versus Aquino model output with X and τ_f parameter identified in open-loop condition. Fixed engine speed and throttle position ($N = 1000$, $P_{man} = 450mbar$). Validation phase.

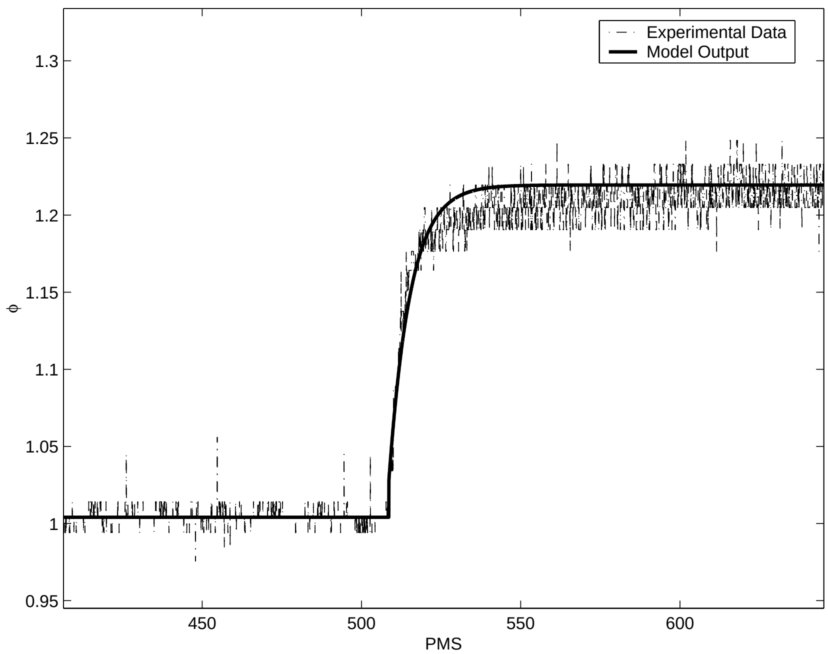

Figure 9: Normalized AIR/FUEL ratio versus Aquino model output with X and τ_f parameter identified in open-loop condition. Fixed engine speed and throttle position ($N = 2000$, $P_{man} = 683mbar$). Validation phase.

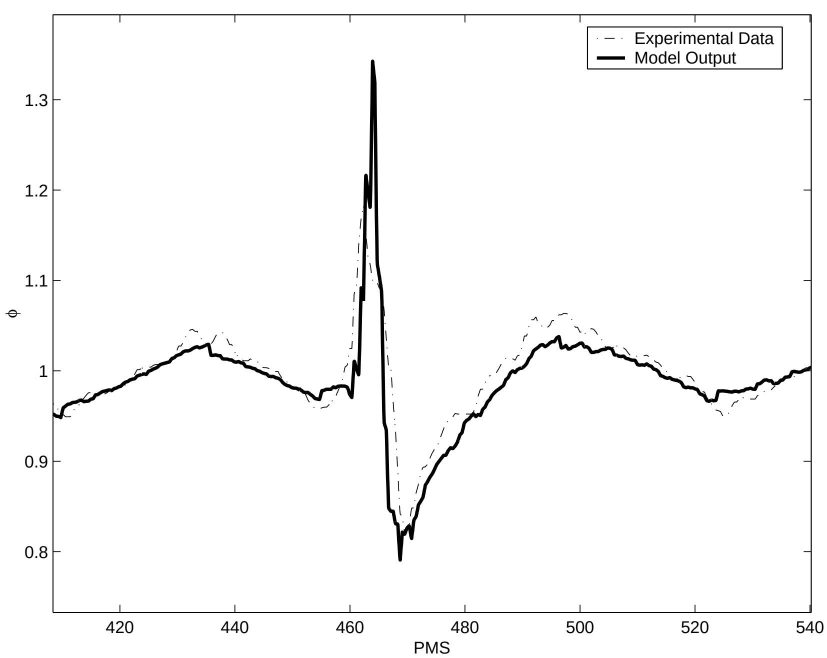

Figure 10: Normalized AIR/FUEL ratio versus Aquino model output with X and τ_f parameter identified in closed-loop condition. Transient condition (see figure 11). Validation phase.

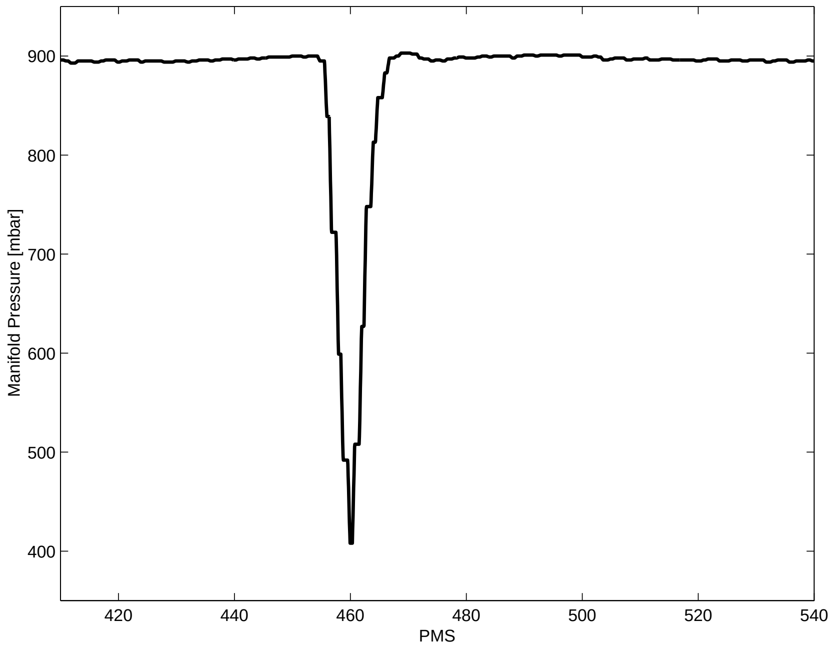

Figure 11: Manifold pressure.

5 Conclusions and Future Work

In this work a procedure for the adaptation of the wall wetting parameters have been presented. The strategy have been tested by simulation, and shows a good behavior in reducing fuel-air excursions during transients. The least square identification procedure have been also tested along experimental data in open-loop and closed-loop conditions.

Future work in this field will concern the test of the proposed strategy on a dynamic test bench and on a vehicle.

References

[1] Aquino, C. F., 'Transient A/F Control Characteristics of the 5 Liter Fuel Injection Engine,' *SAE paper 810494*, 1981.

[2] Chevalier, A., C. W. Vilgid and E. Hendricks, 'Predicting the Port Air Mass Flow of SI Engines in Air/Fuel Ratio Control Applications,' *SAE paper 2000-01-0260*.

[3] Kiencke, U., and L. Nielsen, *Automotive Control Systems*, Springer 2000.

[4] Haluska, P., and L. Guzzella, 'Control-oriented modeling of mixture formation phenomena in multi-port-injection SI gasoline engines', *SAE paper 980628*, 1998.

[5] Hendricks E., T. Vestrholm, P. Kaidantzis, P. Rasmussen, M. Jensen, 'Nonlinear Transient Fuel Film Compensation (NTFC),' *SAE Paper 930767*, 1993.

[6] Hendricks, E., 'Engine Modelling for Control Applications: A Critical Survey,' *Control and Diagnostic in Automotive Applications*, 1996, pp. 357–368.

[7] Heywood J.B., *Internal Combustion Engine Fundamentals*, McGraw-Hill International Editions, 1988.

[8] Johansson, R., *System Modeling and Identification*, Prentice Hall Inc., Englewood Cliffs, New Jersey, 1993.

[9] Ljung, L., *System Identification: Theory for the User*, Prentice Hall Inc., Englewood Cliffs, New Jersey, 1987.

[10] Maloney, P. J., 'An Event Based Transsient Fuel Compensator with Physically Based Parameters,' SAE paper 1999-01-0553, 1999.

[11] Moraal, P. E., D. E. Meyer, J. A. Cook and E. G. Rychlick, 'Adaptive Transient Fuel Compensation: Implementation and Experimental Results,' *SAE paper 2000-01-0550*, 2000.

[12] Onder, C. H., C. A. Roduner, M. R. Simons, and H. P. Geering, 'Wall-Wetting Parameters over the Operating Region of a Sequential Fuel-Injected SI Engine', *SAE paper 98-07-92*, 1998.